Three-phase model of SCIG-based variable speed wind turbine for unbalanced DSLF analysis

Ismail Yusuf, Rudy Gianto
Department of Electrical Engineering, Tanjungpura University, Pontianak, Indonesia

Article Info

ABSTRACT

Steady state performances of the electric power distribution system are normally assessed or evaluated based on load flow analysis. To properly carry out the analysis, a valid steady state load flow model of each distribution system component, including the wind power plant (WPP), needs to be developed. The present paper proposes a method for modeling and integrating squirrel cage induction generator (SCIG)-based variable speed WPP into a three-phase unbalanced distribution system load flow (DSLF) analysis. The proposed method is based on a single-phase T-circuit model of fixed speed WPP, which has successfully been applied to balanced electric power systems. In the present work, the single-phase T-circuit model is extended and modified to be used in steady state load flow analysis of three-phase unbalanced distribution systems embedded with SCIG-based variable speed WPP. Results of the case studies confirm the validity of the proposed method.

Corresponding Author:

Rudy Gianto
Department of Electrical Engineering, Tanjungpura University
St. Prof. Dr. H. Hadari Nawawi, Pontianak 78124, Indonesia
Email: rudy.gianto@ee.untan.ac.id

1. INTRODUCTION

Load or power flow analysis is probably the most fundamental analysis in electric power system studies. Based on the analysis, the steady state performance of the electric power system can be assessed or evaluated. It has been acknowledged that a valid steady state model of each power system component needs to be derived and developed to enable the analysis to correctly be carried out. In the context of wind power plant (WPP) steady state load flow modeling, many methods have been proposed and developed in the last few years. Some of the methods are focused on fixed or near constant speed WPP modeling, and some deal with variable speed WPP modeling.

Several techniques to incorporate fixed speed WPP have been introduced in some publications. The WPP steady state models in [1]–[3] are derived based on the equivalent circuit of the WPP induction generator. Three-node model of an asynchronous generator for load flow analysis has been proposed. The three-node model transforms the asynchronous generator equivalent circuit to several buses and branches [1]–[3]. A standard load flow program is then employed to obtain the load flow solution. A PQ model for an induction generator to be used in steady state load flow analysis has been developed [4]–[6]. The mathematical model in [4]–[6] is derived based on a formula that calculates the active and reactive powers of the induction generator. In the calculation of the powers, the turbine's mechanical power is assumed to be known. Various fixed speed WPP models for steady state load flow analysis have been introduced in [7], [8]. The WPP is modeled under unbalanced system conditions [8]. The developed model in [7] has the power formulations in terms of induction machine parameters, system terminal voltages, and mechanical input power. A method to integrate WPP into

a three-phase load flow analysis has been proposed in [8]. The method in [8] is developed by modifying the single-phase two-port network model so that it can be applied in three-phase systems.

The methods discussed in [1]–[8] can only be applied to fixed speed WPP. Methods for modeling and integrating variable speed WPP have also been proposed and reported in many publications. A load flow model for doubly fed induction generators (DFIGs) is developed [9]. The electric power system and DFIG constraints are simultaneously solved in the model development. Also, in the method [9], the DFIGs are treated as PQ buses, and load flow analysis is carried out to obtain the stator voltages. An iterative technique for integrating DFIG-based WPP for load flow analysis has been introduced in [10]. The technique is based on DFIG steady state equivalent circuit. Moreover, various limits related to the DFIG are also taken into account in the method discussed in [10]. A scheme for incorporating the DFIG-based WPP in distribution systems load flow analysis has been proposed [11]. The proposed model is based on the DFIG equivalent circuit. The DFIGs are treated as PQ buses, and the DFIG reactive power limits are also taken into account in the method [11]. The forward-backward sweep (FBS) technique is then used to obtain the load flow solution of the power system networks [11].

The DFIG model for unbalanced distribution system load flow analysis has been proposed [12]. The model in [12] is derived based on an analytical representation of the WPP major components. The proposed model in [13] is also developed for three-phase load flow analysis. Effects of different rotor speeds are also considered in [13]. Steady state performance analysis of power flow control in DFIG is presented in [14]. Three different rotor speed modes of operation have been included in the analysis [14]. Simple techniques for modeling DFIG-based WPP for power system load flow studies have been proposed in [15]–[17]. In the method [15]–[17], the WPP model is developed based on formulas that calculate the WPP powers. Modeling of a power electronic converter is not needed in the method [15]–[17]. The steady state load flow model of SCIG-based variable speed WPP has been discussed [18]. The model in [18] is also derived based on formulas that calculate the WPP powers. On the other hand, in [19], a model for steady state and dynamic study of a grid-connected SCIG-based WPP has been presented. The model in [19] is established and implemented using MATLAB software.

In most of the methods proposed in [1]-[19], the electric power systems have been assumed to be balanced. As the systems are balanced, single-phase approaches can be used to analyze the systems. It has been acknowledged that power systems are inherently unbalanced. Neglecting the unbalanced, especially if it is of a high level, will lead to invalid and unacceptable results. For such a system, three-phase methods of analysis should be used instead to obtain accurate results. Steady state load flow WPP models for three-phase unbalanced power systems have been introduced [7], [8]. However, the models are only valid for fixed speed WPP and cannot be applied to variable speed WPP. Therefore, against the above background, the present paper proposes a method for modeling and integrating SCIG-based variable speed WPP into a three-phase unbalanced DSLF analysis. The proposed method is based on a single-phase T-circuit model of fixed speed WPP, which has successfully been applied to balanced electric power systems [18]. In the present work, the single-phase T-circuit model is extended and modified to be used in steady state load flow analysis of three-phase unbalanced distribution systems embedded with SCIG-based variable speed WPP. Some case studies are also presented in this paper. In the case study, the validity of the proposed method is investigated and confirmed.

2. THREE-PHASE DSLF PROBLEM FORMULATION

In terms of nodal variables, the formulation of three-phase DSLF problem is given by (1) [8].

$$\{[diag(V^{abc})]^{-1}(S_G^{abc} - S_L^{abc})\}^* - Y^{abc}V^{abc} = 0 \tag{1}$$

where V^{abc} is nodal voltage vector, S_G^{abc} is power injection (generation) vector, S_L^{abc} is power demand vector (load), and Y^{abc} is power system nodal admittance matrix. In (1), V^{abc}, S_G^{abc}, S_L^{abc}, and Y^{abc} are of the forms:

$$V^{abc} = [V_1^{abc} \quad V_2^{abc} \quad \cdots \quad V_n^{abc}]^T \tag{2}$$

$$S_G^{abc} = [S_{G1}^{abc} \quad S_{G2}^{abc} \quad \cdots \quad S_{Gn}^{abc}]^T \tag{3}$$

$$S_L^{abc} = [S_{L1}^{abc} \quad S_{L2}^{abc} \quad \cdots \quad S_{Ln}^{abc}]^T \tag{4}$$

$$Y^{abc} = \begin{bmatrix} Y_{11}^{abc} & Y_{12}^{abc} & \cdots & Y_{1n}^{abc} \\ Y_{21}^{abc} & Y_{22}^{abc} & \vdots & Y_{2n}^{abc} \\ \vdots & \vdots & \ddots & \vdots \\ Y_{n1}^{abc} & Y_{n2}^{abc} & \cdots & Y_{nn}^{abc} \end{bmatrix} \tag{5}$$

where n is the number of power system nodes, and:

$$V_i^{abc} = [V_i^a \quad V_i^b \quad V_i^c]^T \tag{6}$$

$$S_{Gi}^{abc} = [S_{Gi}^a \quad S_{Gi}^b \quad S_{Gi}^c]^T \tag{7}$$

$$S_{Li}^{abc} = [S_{Li}^a \quad S_{Li}^b \quad S_{Li}^c]^T \tag{8}$$

$$Y_{ii}^{abc} = \begin{bmatrix} Y_{ii}^{aa} & Y_{ii}^{ab} & Y_{ii}^{ac} \\ Y_{ii}^{ba} & Y_{ii}^{bb} & Y_{ii}^{bc} \\ Y_{ii}^{ca} & Y_{ii}^{cb} & Y_{ii}^{cc} \end{bmatrix} \tag{9}$$

$$Y_{ij}^{abc} = \begin{bmatrix} Y_{ij}^{aa} & Y_{ij}^{ab} & Y_{ij}^{ac} \\ Y_{ij}^{ba} & Y_{ij}^{bb} & Y_{ij}^{bc} \\ Y_{ij}^{ca} & Y_{ij}^{cb} & Y_{ij}^{cc} \end{bmatrix} \tag{10}$$

In conventional DSLF analysis, power system nodes can be classified into two categories, namely: substation and load nodes. In the analysis, the substation node is usually considered the reference node. Therefore, this node's voltage magnitude and angle are specified at some values. The substation voltage magnitude is generally set at 1.0 pu (or a value near 1.0 pu), and the substation voltage angle is assumed to be zero (reference node). Since the distribution system is typically fed from the substation, the remaining nodes in the system can be considered load nodes. Therefore, the power generation of these nodes is all zeroes (see Table 1).

Table 1. Known and unknown quantities

Node	Known quantity	Unknown quantity
Substation	$V^{abc} = \begin{bmatrix} 1.0\angle 0^o \\ 1.0\angle -120^o \\ 1.0\angle 120^o \end{bmatrix}$	S_G^{abc}
Load	$S_G^{abc} = [0 \quad 0 \quad 0]^T$	V^{abc}

3. MODEL OF SCIG-BASED VARIABLE SPEED WIND TURBINE

It has been acknowledged that variable speed wind turbines can harness wind energy more efficiently than fixed speed wind turbines. This advantage is probably the main reason why variable speed wind turbines have been replacing fixed speed wind turbines in the last few decades. Several configurations can be used to implement the variable speed operation of a wind turbine. However, due to its relatively lower cost and easy maintenance, the SCIG-based variable speed wind turbine is gaining popularity nowadays.

Figure 1 shows a basic structure of a SCIG-based variable speed wind turbine system [18]–[23]. It can be seen from Figure 1 that the main component of the system is SCIG which converts turbine mechanical power to electrical power. The system also contains a power electronic converter (PEC), which consists of a power converter/inverter, and a DC-link. The PEC will isolate the SCIG speed from the frequency of the power grid where the WPP is connected. This isolation makes the WPP operation speeds wider, and the wind energy can be extracted more efficiently. Moreover, with the presence of PEC, the WPP can be set to control the reactive power output and support the system's reactive power demand.

The equivalent circuit of SCIG is shown in Figure 2 [18]–[23]. In Figure 2, the electrical quantities V_S, I_S, V_R, and I_R denote stator voltage, stator current, rotor voltage, and rotor current, respectively. The circuit impedances Z_S, Z_R, and Z_M in the figure are determined using:

$$Z_S = R_S + jX_S \tag{11}$$

$$Z_R = R_R + jX_R \tag{12}$$

$$Z_M = jR_cX_m/(R_c + jX_m) \tag{13}$$

where R_S, X_S, R_R, X_R, R_c, and X_m are the stator circuit resistance, stator circuit reactance, rotor circuit resistance, rotor circuit reactance, magnetic core circuit resistance, and magnetic core circuit reactance, respectively.
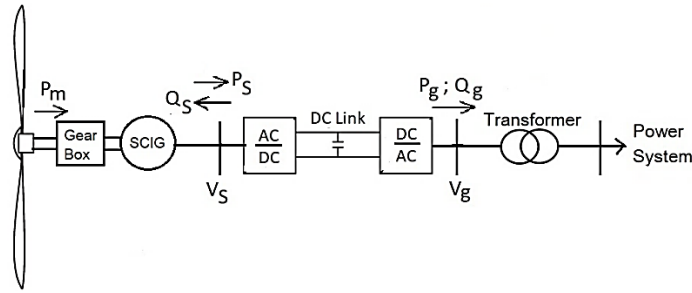
Figure 1. Structure of SCIG-based variable speed wind turbine
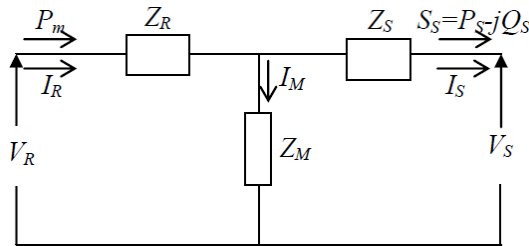
Figure 2. Steady state equivalent circuit of SCIG

In [18], it has been shown that a single-phase steady state model of SCIG-based variable speed WPP valid for a load flow analysis of a balanced power system is of the form:

$$Z_{T1}V_v + Z_{T2}S_S + Z_{T3}S_S^* + Z_{T4}S_v - P_m = 0 \tag{14}$$

where:

$$V_v = \frac{V_g V_g^*}{\eta_c^2} \tag{15}$$

$$S_v = \frac{\eta_c^2 S_S S_S^*}{V_g V_g^*} \tag{16}$$

$$Z_{T1} = \frac{1}{Z_{M*}} + \frac{Z_R}{Z_M Z_{M*}} \tag{17}$$

$$Z_{T2} = 1 + \frac{Z_S^*}{Z_M^*} + \frac{Z_R}{Z_M} + \frac{Z_S^* Z_R}{Z_M Z_M^*} \tag{18}$$

$$Z_{T3} = \frac{Z_S}{Z_M^*} + \frac{Z_S Z_R}{Z_M Z_M^*} + \frac{Z_R}{Z_M^*} \tag{19}$$

$$Z_{T4} = Z_S + Z_R + \frac{Z_S Z_S^*}{Z_M^*} + \frac{Z_S Z_R}{Z_M} + \frac{Z_S Z_S^* Z_R}{Z_M Z_M^*} + \frac{Z_S^* Z_R}{Z_M^*} \tag{20}$$

In (15) and (16), η_c is the PEC efficiency. It is to be noted that the power injection (i.e., power generation) at the WPP bus is also the WPP power output. In the present work, it will be assumed that the WPP is operated at a unity power factor, i.e., there is no reactive power delivered/absorbed to/from the power system ($Q_g = 0$). Therefore, power injection at the WPP bus is:

$$S_G = P_g = \eta_c P_S \tag{21}$$

4. THREE-PHASE MODEL OF SCIG-BASED VARIABLE SPEED WIND TURBINE

To facilitate the load flow analysis in a three-phase system, the WPP single-phase model (14) is extended to become:

$$Z_{T1}^{abc}V_v^{abc} + Z_{T2}^{abc}S_S^{abc} + Z_{T3}^{abc}(S_S^{abc})^* + Z_{T4}^{abc}S_v^{abc} - P_m^{abc} = 0 \tag{22}$$

where:

$$P_m^{abc} = \begin{bmatrix} \frac{P_m}{3} & \frac{P_m}{3} & \frac{P_m}{3} \end{bmatrix}^T \tag{23}$$

$$S_S^{abc} = \begin{bmatrix} S_S^a & S_S^b & S_S^c \end{bmatrix}^T \tag{24}$$

$$V_v^{abc} = \frac{1}{\eta_c^2} \begin{bmatrix} V_g^a (V_g^a)^* & V_g^b (V_g^b)^* & V_g^b (V_g^b)^* \end{bmatrix}^T \tag{25}$$

$$S_v^{abc} = \eta_c^2 \begin{bmatrix} \frac{s_S^a (s_S^a)^*}{v_g^a (v_g^a)^*} & \frac{s_S^b (s_S^b)^*}{v_g^b (v_g^b)^*} & \frac{s_S^c (s_S^c)^*}{v_g^c (v_g^c)^*} \end{bmatrix}^T \tag{26}$$

$$Z_{Ti}^{abc} = \begin{bmatrix} Z_{Ti}^a & 0 & 0 \\ 0 & Z_{Ti}^b & 0 \\ 0 & 0 & Z_{Ti}^c \end{bmatrix}; i = 1,2,3,4 \tag{27}$$

In (27), the $Z_{Ti}{}^{abc}$ sub-matrices are determined based on (17) - (20) as:

$$Z_{T1}^p = \frac{1}{(z_M^p)^*} + \frac{z_R^p}{z_M^p (z_M^p)^*} \tag{28}$$

$$Z_{T2}^p = 1 + \frac{(z_S^p)^*}{(z_M^p)^*} + \frac{z_R^p}{z_M^p} + \frac{(z_S^p)^* z_R^p}{z_M^p (z_M^p)^*} \tag{29}$$

$$Z_{T3}^p = \frac{z_S^p}{(z_M^p)^*} + \frac{z_S^p z_R^p}{z_M^p (z_M^p)^*} + \frac{z_R^p}{(z_M^p)^*} \tag{30}$$

$$Z_{T4}^p = Z_S^p + Z_R^p + \frac{z_S^p (z_S^p)^*}{(z_M^p)^*} + \frac{z_S^p z_R^p}{z_M^p} + \frac{z_S^p (z_S^p)^* z_R^p}{z_M^p (z_M^p)^*} + \frac{(z_S^p)^* z_R^p}{(z_M^p)^*} \tag{31}$$

where $p = a, b, c$. In (28) - (31), $Z_S{}^p$, $Z_R{}^p$, and $Z_M{}^p$ are calculated based on (11) - (13) as:

$$Z_S^p = R_S^p + jX_S^p \tag{32}$$

$$Z_R^p = R_R^p + jX_R^p \tag{33}$$

$$Z_M^p = jR_c^p X_m^p / (R_c^p + jX_m^p) \tag{34}$$

According to (1) and (22) represent the complete formulation of the three-phase load flow problem of the electric power distribution system embedded with SCIG-based variable speed WPP. The quantities to be calculated and the equations to be solved are given in Table 2. By looking at Figure 1, it is clear that at the WPP node, the following relationships are valid:

$$V_i^{abc} = V_g^{abc} \tag{35}$$

$$S_{Gi}^{abc} = S_g^{abc} = \eta_c P_S^{abc} \tag{36}$$

where:

$$V_g^{abc} = \begin{bmatrix} V_g^a & V_g^b & V_g^c \end{bmatrix}^T \tag{37}$$

$$S_g^{abc} = \begin{bmatrix} S_g^a & S_g^b & S_g^c \end{bmatrix}^T \tag{38}$$

$$P_S^{abc} = \begin{bmatrix} P_S^a & P_S^b & P_S^c \end{bmatrix}^T \tag{39}$$

Table 2. Known and unknown quantities for system with WPP

Node	Equation	Known quantity	Unknown quantity
Substation	(1)	$V^{abc} = \begin{bmatrix} 1.0\angle 0^o \\ 1.0\angle -120^o \\ 1.0\angle 120^o \end{bmatrix}$	S_G^{abc}
Load	(1)	$S_G^{abc} = [0 \quad 0 \quad 0]^T$	V^{abc}
WPP	(1) & (22)	$P_m^{abc}; Z_S^p; Z_R^p; Z_M^p$	$V^{abc}; S_S^{abc}$

5. CASE STUDY
5.1. Case study 1
5.1.1. Test system

To confirm the method proposed in section 4, a 12-node balanced distribution system shown in Figure 3 will be used in this first case study [24], [25]. Although the system is balanced and can be analysed by single-phase approach, for the purpose of validation study, it will be analysed using the proposed three-phase method. The system voltage in Figure 3 is 11 kV with a total three-phase load of 4.305 kW and 1.215 kVAR. The system data is presented in Table 3. In this case study, WPP with a power rating of 3.5 MW is assumed to be connected to node 12 via a step-up transformer. Data of the WPP is given in Table 4. All data in pu are on 1 MVA base.

5.1.2. Turbine mechanical power

It has been acknowledged that turbine mechanical power (P_m) depends highly on the wind speed. Table 5 shows the amount of turbine mechanical powers for various wind speeds used in the first case study. The turbine powers have been calculated using the formula given in [15]. In the calculation, the values of air density and turbine performance coefficient are assumed to be 1.225 kg/m^3 and 0.45, respectively.

5.1.3. Results and discussion

Tables 6-9 present the results of the load flow analysis for the 12-node distribution system. Because the system is balanced, electric quantities in the three phases are all identical. It can be seen that the results in Tables 6–9 are in excellent agreement with the results in [18] which confirm the proposed method validity.
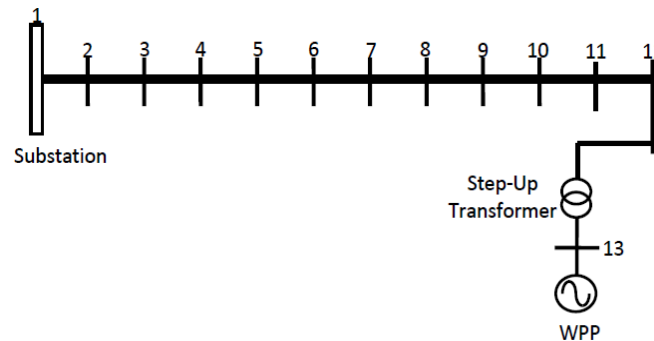
Figure 3. Test system (12-node network)

Table 3. Test system data (12-node network)

Line No.	Sending Bus	Receiving Bus	R*	X*	P_L**	Q_L**
1	1	2	1.093	0.455	60	60
2	2	3	1.184	0.494	140	30
3	3	4	2.095	0.873	155	55
4	4	5	3.188	1.329	130	30
5	5	6	1.093	0.455	120	15
6	6	7	1.002	0.417	155	55
7	7	8	4.403	1.215	145	45
8	8	9	5.642	1.597	140	40
9	9	10	2.890	0.818	135	30
10	10	11	1.514	0.428	140	30
11	11	12	1.238	0.351	115	15

*Line resistance/reactance in ohm/phase
**Load connected to receiving bus in kW and kVAR (perphase)

Table 4. WPP data (12-node network)

Component	Quantity
Turbine	Blade length: 45 meter
	Rated power: 3.5 MW
	Speed:
	Cut-in: 5 m/s; Rated: 12 m/s; Cut-out: 23 m/s
Gear Box	Ratio: 1/60
Generator	Type: SCIG
	Rated power: 3.5 MW
	Pole pairs: 4
	Voltage: 690 Volt
	Resistances/Reactances (in pu):
	$R_s^a = R_s^b = R_s^c = R_r^a = R_r^b = R_r^c = 0.01$
	$X_s^a = X_s^b = X_s^c = X_r^a = X_r^b = X_r^c = 0.10$
	$R_c^a = R_c^b = R_c^c = 500, X_m^a = X_m^b = X_m^c = 50$
PEC	Efficiency: 95%
Step-Up Transformer	Impedance (in pu*): $Z^a = Z^b = Z^c = j0.1$

Table 5. Turbine power (12-node network)

Wind Speed (m/s)	Turbine power (MW)
5	0.3367
6	0.5346
7	0.7980
8	1.3362
9	1.5586
10	2.0745
11	2.6933
12	3.4243

Table 6. Power output of WPP (12-node network)

P_m (MW)	Phase-a (MW)	Phase-b (MW)	Phase-c (MW)	3-Phase (MW)
0.3367	0.1035	0.1035	0.1035	0.3105
0.5346	0.1640	0.1640	0.1640	0.4920
0.7980	0.2435	0.2435	0.2435	0.7305
1.3362	0.4023	0.4023	0.4023	1.2069
1.5586	0.4668	0.4668	0.4668	1.4004
2.0745	0.6140	0.6140	0.6140	1.8420
2.6933	0.7868	0.7868	0.7868	2.3604
3.4243	0.9862	0.9862	0.9862	2.9586

Table 7. WPP terminal voltage magnitude (12-node network)

P_m (MW)	Phase-a (pu)	Phase-b (pu)	Phase-c (pu)
0.3367	0.8902	0.8902	0.8902
0.5346	0.9059	0.9059	0.9059
0.7980	0.9254	0.9254	0.9254
1.3362	0.9614	0.9614	0.9614
1.5586	0.9751	0.9751	0.9751
2.0745	1.0045	1.0045	1.0045
2.6933	1.0363	1.0363	1.0363
3.4243	1.0701	1.0701	1.0701

Table 8. Distribution line loss (12-node network)

P_m (MW)	Phase-a (MW, MVAR)	Phase-b (MW, MVAR)	Phase-c (MW, MVAR)	3-Phase (MW, MVAR)
0.3367	0.1418+j0.0563	0.1418+j0.0563	0.1418+j0.0563	0.4254+j0.1689
0.5346	0.1206+j0.0504	0.1206+j0.0504	0.1206+j0.0504	0.3618+j0.1512
0.7980	0.0976+j0.0455	0.0976+j0.0455	0.0976+j0.0455	0.2928+j0.1365
1.3362	0.0650+j0.0436	0.0650+j0.0436	0.0650+j0.0436	0.1950+j0.1308
1.5586	0.0561+j0.0454	0.0561+j0.0454	0.0561+j0.0454	0.1683+j0.1362
2.0745	0.0438+j0.0545	0.0438+j0.0545	0.0438+j0.0545	0.1314+j0.1635
2.6933	0.0416+j0.0726	0.0416+j0.0726	0.0416+j0.0726	0.1248+j0.2178
3.4243	0.0726+j0.1021	0.0726+j0.1021	0.0726+j0.1021	0.1578+j0.3063

Table 9. Substation power (12-node network)

P_m (MW)	Phase-a (MW, kVAR)	Phase-b (MW, MVAR)	Phase-c (MW, MVAR)	3-Phase (MW, MVAR)
0.3367	1.4733+j0.4613	1.4733+j0.4613	1.4733+j0.4613	4.4199+j1.3839
0.5346	1.3916+j0.4554	1.3916+j0.4554	1.3916+j0.4554	4.1748+j1.3662
0.7980	1.2891+j0.4505	1.2891+j0.4505	1.2891+j0.4505	3.8673+j1.3515
1.3362	1.0977+j0.4486	1.0977+j0.4486	1.0977+j0.4486	3.2931+j1.3458
1.5586	1.0243+j0.4504	1.0243+j0.4504	1.0243+j0.4504	3.0729+j1.3512
2.0745	0.8648+j0.4595	0.8648+j0.4595	0.8648+j0.4595	2.5944+j1.3785
2.6933	0.6897+j0.4776	0.6897+j0.4776	0.6897+j0.4776	2.0691+j1.4328
3.4243	0.5015+j0.5071	0.5015+j0.5071	0.5015+j0.5071	1.5045+j1.5213

5.2. Case study 2
5.2.1. Test system
To further validate the method proposed in section 4, a 19-node unbalanced distribution system shown in Figure 4 will be used in this case study [24], [25]. The system voltage in Figure 4 is 11 kV with a total three-phase load of 515.94 kW and 177.27 kVAR (Phase-a: 176.33 kW and 61.23 kVAR; Phase-b: 166.34 kW and 56.34 kVAR; Phase-c: 173.27 kW and 59.70 kVAR). The system data is presented in Tables 10 and 11. In this case study, WPP with a power rating of 300 kW is assumed to be connected to node 19 via a step-up transformer. Data of the WPP is given in Table 12. All data in pu are on 1 MVA base.

5.2.2. Turbine mechanical power
Table 13 shows the turbine mechanical powers for various wind speeds used in the second case study. The turbine powers have also been calculated using the formula given in [15]. In the calculation, the values of air density and turbine performance coefficient are assumed to be 1.225 kg/m^3 and 0.35, respectively.
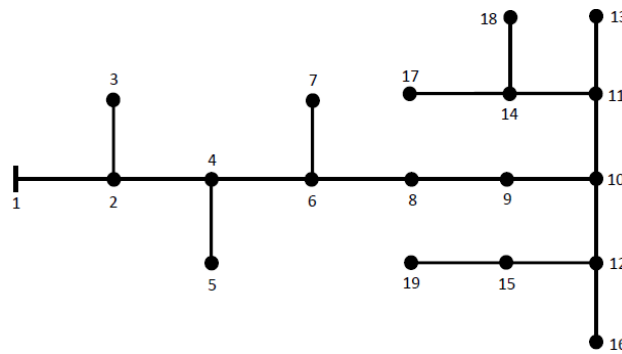
Figure 4. Test system (19-node network)

Table 10. Test system line data (19-node network)

No.	Line	Self-impedance (Ohm)	Mutual impedance (Ohm)
1	1 − 2	3.0×(1.56090+j0.67155)	3.0×(0.52030+j0.22385)
2	2 − 3	5.0×(1.56090+j0.67155)	5.0×(0.52030+j0.22385)
3	2 − 4	1.5×(1.56090+j0.67155)	1.5×(0.52030+j0.22385)
4	4 − 5	1.5×(1.56090+j0.67155)	1.5×(0.52030+j0.22385)
5	4 − 6	1.0×(1.56090+j0.67155)	1.0×(0.52030+j0.22385)
6	6 − 7	2.0×(1.56090+j0.67155)	2.0×(0.52030+j0.22385)
7	6 − 8	2.5×(1.56090+j0.67155)	2.5×(0.52030+j0.22385)
8	8 − 9	3.0×(1.56090+j0.67155)	3.0×(0.52030+j0.22385)
9	9 − 10	5.0×(1.56090+j0.67155)	5.0×(0.52030+j0.22385)
10	10 − 11	1.5×(1.56090+j0.67155)	1.5×(0.52030+j0.22385)
11	10 − 12	1.5×(1.56090+j0.67155)	1.5×(0.52030+j0.22385)
12	11 − 13	5.0×(1.56090+j0.67155)	5.0×(0.52030+j0.22385)
13	11 − 14	1.0×(1.56090+j0.67155)	1.0×(0.52030+j0.22385)
14	12 − 15	5.0×(1.56090+j0.67155)	5.0×(0.52030+j0.22385)
15	12 − 16	6.0×(1.56090+j0.67155)	6.0×(0.52030+j0.22385)
16	14 − 17	3.5×(1.56090+j0.67155)	3.5×(0.52030+j0.22385)
17	14 − 18	4.0×(1.56090+j0.67155)	4.0×(0.52030+j0.22385)
18	15 − 19	4.0×(1.56090+j0.67155)	4.0×(0.52030+j0.22385)

Table 11. Test system load data (19-node network)

Node	Phase-a		Phase-b		Phase-c	
	P (kW)	Q (kVAR)	P (kW)	Q (kVAR)	P (kW)	Q (kVAR)
1	0	0	0	0	0	0
2	10.38	5.01	5.19	2.52	10.38	5.01
3	11.01	5.34	5.19	2.52	9.72	4.71
4	4.05	1.95	5.67	2.76	6.48	3.15
5	6.48	3.15	5.19	2.52	4.53	2.19
6	4.20	2.04	3.09	1.50	2.91	1.41
7	9.72	4.71	8.10	3.93	8.10	3.93
8	7.44	3.60	5.34	2.58	3.39	1.65
9	12.30	5.97	14.91	7.23	13.29	6.42
10	3.39	1.65	4.20	2.04	2.58	1.26
11	7.44	3.60	7.44	3.60	11.01	5.34
12	9.72	4.71	8.10	3.93	8.10	3.93
13	4.38	2.13	5.34	2.58	6.48	3.15
14	3.09	1.50	3.09	1.50	4.05	1.95
15	14.38	2.13	14.86	2.34	16.96	3.36
16	17.77	3.78	20.38	5.01	17.77	3.78
17	16.48	3.15	14.86	2.34	14.86	2.34
18	15.34	2.58	15.34	2.58	15.52	2.67
19	18.76	4.23	20.05	4.86	17.14	3.45

Table 12. WPP data (19-node network)

Component	Quantity
Turbine	Blade length: 16 meter
	Rated power: 300 kW
	Speed:
	Cut-in: 5 m/s; Rated: 12 m/s; Cut-out: 23 m/s
Gear Box	Ratio: 1/40
Generator	Type: SCIG
	Rated power: 300 kW
	Pole pairs: 2
	Voltage: 690 Volt
	Resistances/Reactances (in pu):
	$R_s^a = R_s^b = R_s^c = R_r^a = R_r^b = R_r^c = 0.0020$
	$X_s^a = X_s^b = X_s^c = X_r^a = X_r^b = X_r^c = 0.0100$
	$R_c^a = R_c^b = R_c^c = 500, X_m^a = X_m^b = X_m^c = 25$
PEC	Efficiency: 95%
Step-Up Transformer	Impedance (in pu*): $Z^a = Z^b = Z^c = j0.1$

Table 13. Turbine power (19-node network)

Wind Speed (m/s)	Turbine Power (kW)	Wind Speed (m/s)	Turbine Power (kW)
5	21.5513	9	125.6873
6	37.2407	10	172.4106
7	59.1368	11	229.4785
8	88.2742	12	297.9255

5.2.3. Results and discussion

Tables 14-17 present the results of the load flow analysis for the 19-node distribution system. Because the system is unbalanced, it can be seen that the electric quantities in the three phases are not the same. The results of the load flow analysis also show that with the increase in turbine mechanical power input, the WPP active power output also increases (see Table 14 and Figure 5). However, its value is slightly smaller than the mechanical power due to power losses in the WPP (i.e., losses in SCIG and PEC).

With the installation of WPP, one of the advantages is that the system voltage profile can be improved (see Table 15 and Figure 6). This improvement is caused by the WPP power injection. It can be seen that the voltage profile gets better with the increase in WPP power injection (i.e., WPP output). The system voltage profile improvement will, in turn, reduce the distribution line power losses as the power injection increases (see Table 16 and Figure 7). Another important advantage obtained with the presence of WPP is that the power supplied by the substation can be reduced (see Table 17 and Figure 8). The reduction in substation power is possible because some of the system loads can be fed by the WPP. It is also to be observed that for every case of turbine power value, the substation power plus WPP power always equals total system load plus distribution line losses. It is to be noted that the line losses have been calculated based on the line impedances and currents. These results further verify the validity of the method proposed.

Table 14. Power output of WPP (19-node network)

P_m (kW)	Phase-a (kW)	Phase-b (kW)	Phase-c (kW)	3-Phase (kW)
21.5513	5.01	5.02	5.02	15.05
37.2407	9.97	9.97	9.97	29.91
59.1368	16.88	16.89	16.88	50.65
88.2742	26.08	26.08	26.08	78.24
125.6873	37.89	37.89	37.89	113.67
172.4106	52.63	52.64	52.64	157.91
229.4785	70.65	70.65	70.65	211.95
297.9255	92.24	92.25	92.25	276.74

Table 15. WPP terminal voltage magnitude (19-node network)

P_m (kW)	Phase-a (pu)	Phase-b (pu)	Phase-c (pu)
21.5513	0.92691	0.92492	0.92565
37.2407	0.93075	0.92879	0.92951
59.1368	0.93604	0.93412	0.93482
88.2742	0.94298	0.94111	0.94179
125.6873	0.95171	0.94990	0.95056
172.4106	0.96237	0.96062	0.96125
229.4785	0.97502	0.97335	0.97394
297.9255	0.98971	0.98812	0.98868

Table 16. Distribution line loss (19-node network)

P_m (kW)	Phase-a (kW, kVAR)	Phase-b (kW, kVAR)	Phase-c (kW, kVAR)	3-Phase (kW, kVAR)
21.5513	9.57+j4.16	9.68+j4.12	9.81+j4.23	29.06+j12.51
37.2407	8.85+j3.86	8.95+j3.82	9.08+j3.92	26.88+j11.60
59.1368	7.94+j3.48	8.00+j3.44	8.14+j3.54	24.08+j10.46
88.2742	6.86+j3.06	6.89+j3.01	7.04+j3.10	20.78+j9.17
125.6873	5.70+j2.64	5.69+j2.58	5.85+j2.67	17.24+j7.89
172.4106	4.58+j2.31	4.53+j2.23	4.71+j2.31	13.83+j6.85
229.4785	3.70+j2.15	3.60+j2.07	3.79+j2.13	11.09+j6.35
297.9255	3.28+j2.31	3.12+j2.22	3.34+j2.27	9.74+j6.80

Three-phase model of SCIG-based variable speed wind turbine for unbalanced DSLF … (Ismail Yusuf)

Table 17. Substation power (19-node network)

P_m (kW)	Phase-a (kW, kVAR)	Phase-b (kW, kVAR)	Phase-c (kW, kVAR)	3-Phase (kW, kVAR)
21.5513	180.89+j65.39	171.00+j60.46	178.06+j63.93	529.94+j189.78
37.2407	175.22+j65.09	165.31+j60.16	172.38+j63.62	512.90+j188.87
59.1368	167.39+j64.71	157.45+j59.78	164.53+j63.24	489.37+j187.73
88.2742	157.11+j64.29	147.14+j59.35	154.23+j62.80	458.48+j186.44
125.6873	144.14+j63.87	134.13+j58.92	141.23+j62.37	419.51+j185.16
172.4106	128.28+j63.54	118.23+j58.57	125.34+j62.01	371.85+j184.12
229.4785	109.38+j63.38	99.28+j58.41	106.41+j61.83	315.08+j183.62
297.9255	87.36+j63.54	77.21+j58.56	84.36+j61.97	248.93+j184.07
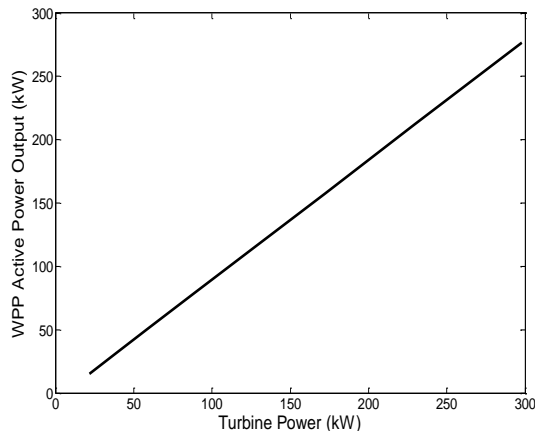
Figure 5. Variation of WPP active power output
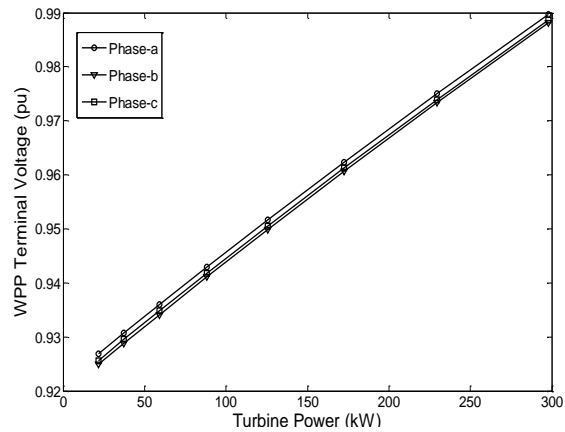
Figure 6. Variation of WPP terminal voltage
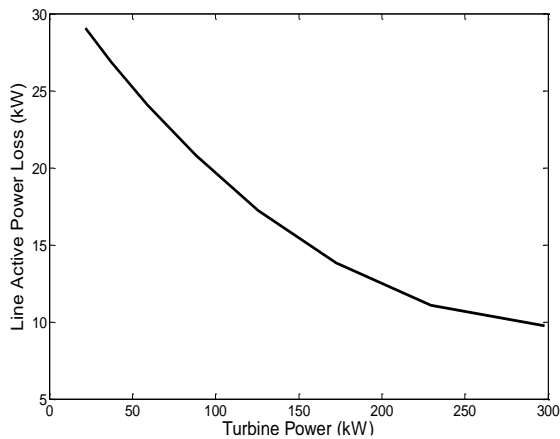
Figure 7. Variation of line active power loss
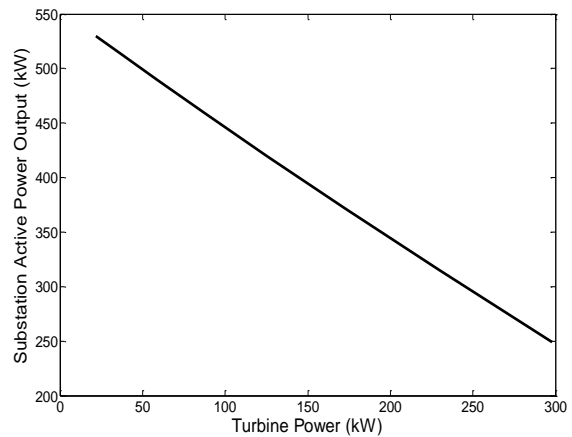
Figure 8. Variation of substation active power output

6. CONCLUSION

A method for modeling and integrating SCIG-based variable speed WPP into three-phase unbalanced DSLF analysis has been proposed in this paper. The method is based on a single-phase T-circuit model of fixed speed WPP, which has successfully been applied to balanced electric power systems. In the present work, the single-phase T-circuit model is extended and modified so that can be applied in steady state load flow analysis of three-phase unbalanced distribution systems embedded with SCIG-based variable speed WPP. Case studies have also been presented in this paper. In the case studies, validity of the proposed method is investigated and confirmed. Results of the case studies also demonstrate the capability of the proposed method in representing the SCIG-based variable speed WPP for steady state load flow studies of the electric power distribution systems.

REFERENCES

[1]   M. H. Haque, "Evaluation of power flow solutions with fixed speed wind turbine generating systems," *Energy Conversion and Management*, vol. 79, pp. 511–518, Mar. 2014, doi: 10.1016/j.enconman.2013.12.049.

[2]   J. Wang, C. Huang, and A. F. Zobaa, "Multiple-node models of asynchronous wind turbines in wind farm for load flow analysis," *Electric Power Components and Systems*, vol. 44, no. 2, pp. 135–141, Jan. 2016, doi: 10.1080/15325008.2015.1102180.

[3]   M. H. Haque, "Incorporation of fixed speed wind turbine generators in load flow analysis of distribution systems," *International Journal of Renewable Energy Technology*, vol. 6, no. 4, p. 317, 2015, doi: 10.1504/ijret.2015.072099.

[4]   A. Feijoo, J. Luis Pazos, and D. Villanueva, "Conventional asynchronous wind turbine models mathematical expressions for the load flow analysis," *International Journal of Energy Engineering*, vol. 3, no. 6, pp. 269–278, Dec. 2013, doi: 10.5963/ijee0306008.

[5]   A. Feijoo and D. Villanueva, "A PQ model for asynchronous machines based on rotor voltage calculation," *IEEE Transactions on Energy Conversion*, vol. 31, no. 2, pp. 813–814, 2016, doi: 10.1109/TEC.2016.2529502.

[6]   A. Feijoo and D. Villanueva, "Erratum: A PQ model for asynchronous machines based on rotor voltage calculation (IEEE Transactions on Energy Conversion (2016) 31: 2 (813-814) DOI: 10.1109/TEC.2016.2529502)," *IEEE Transactions on Energy Conversion*, vol. 31, no. 3, p. 1228, Sep. 2016, doi: 10.1109/TEC.2016.2592758.

[7]   A. Koksoy, O. Ozturk, M. E. Balci, and M. H. Hocaoglu, "A newwind turbine generating system model for balanced and unbalanced distribution systems load flow analysis," *Applied Sciences (Switzerland)*, vol. 8, no. 4, p. 502, Mar. 2018, doi: 10.3390/app8040502.

[8]   R. Gianto and Purwoharjono, "Two-port network model of wind turbine generator for three-phase unbalanced distribution system load flow analysis," *Bulletin of Electrical Engineering and Informatics (BEEI)*, vol. 11, no. 1, pp. 9–19, Feb. 2022, doi: 10.11591/eei.v11i1.3074.

[9]   S. Li, "Power flow modeling to doubly-fed induction generators (DFIGs) under power regulation," *IEEE Transactions on Power Systems*, vol. 28, no. 3, pp. 3292–3301, Aug. 2013, doi: 10.1109/TPWRS.2013.2251914.

[10]   V. Seshadri Sravan Kumar and D. Thukaram, "Accurate modeling of doubly fed induction generator based wind farms in load flow analysis," *Electric Power Systems Research*, vol. 155, pp. 363–371, Feb. 2018, doi: 10.1016/j.epsr.2017.09.011.

[11]   A. C. V. S. and V. Seshadri Sravan Kumar, "Enhanced modelling of doubly fed induction generator in load flow analysis of distribution systems," *IET Renewable Power Generation*, vol. 15, no. 5, pp. 980–989, Apr. 2021, doi: 10.1049/rpg2.12077.

[12]   A. Dadhania, B. Venkatesh, A. B. Nassif, and V. K. Sood, "Modeling of doubly fed induction generators for distribution system power flow analysis," *International Journal of Electrical Power and Energy Systems*, vol. 53, no. 1, pp. 576–583, Dec. 2013, doi: 10.1016/j.ijepes.2013.05.025.

[13]   Y. Ju, F. Ge, W. Wu, Y. Lin, and J. Wang, "Three-phase steady-state model of doubly fed induction generator considering various rotor speeds," *IEEE Access*, vol. 4, pp. 9479–9488, 2016, doi: 10.1109/ACCESS.2016.2646683.

[14]   C. M. Nwosu, S. E. Oti, and C. U. Ogbuka, "Transient and steady state performance analysis of power flow control in a DFIG variable speed wind turbine," *Journal of Electrical Engineering*, vol. 68, no. 1, pp. 31–38, Jan. 2017, doi: 10.1515/jee-2017-0004.

[15]   R. Gianto, "Steady-state model of DFIG-based wind power plant for load flow analysis," *IET Renewable Power Generation*, vol. 15, no. 8, pp. 1724–1735, Jun. 2021, doi: 10.1049/rpg2.12141.

[16]   R. Gianto, "Constant power factor model of DFIG-based wind turbine for steady state load flow studies," *Energies*, vol. 15, no. 16, p. 6077, Aug. 2022, doi: 10.3390/en15166077.

[17]   R. Gianto, Purwoharjono, F. Imansyah, R. Kurnianto, and Danial, "Steady-state load flow model of DFIG wind turbine based on generator power loss calculation," *Energies*, vol. 16, no. 9, p. 3640, Apr. 2023, doi: 10.3390/en16093640.

[18]   R. Gianto and A. Elbani, "Modeling of SCIG-based variable speed wind turbine in power factor control mode for load flow analysis," *European Journal of Electrical Engineering and Computer Science*, vol. 5, no. 6, pp. 43–48, Dec. 2021, doi: 10.24018/ejece.2021.5.6.378.

[19]   M. Benchagra, M. Ouassaid, M. Hilal, Y. Errami, and M. Maaroufi, "Modeling and control of SCIG based variable speed with power factor control," *International Review on Modelling and Simulations (IREMOS)*, vol. 4, no. 3, pp. 1007–1014, 2011.

[20]   V. Akhmatov, *Induction generators for wind power*, vol. 0. Multi-Science Publishing Co. Ltd., 2007.

[21]   I. Boldea, *Variable Speed Generators*. CRC Press, 2015, doi: 10.1201/b19293.

[22]   O. Anaya-Lara, N. Jenkins, J. B. Ekanayake, P. Cartwright, and M. Hughes, *Wind energy generation: modelling and control*. John Wiley & Sons Ltd, 2009.

[23]   T. Ackermann, *Wind power in power systems*. Wiley, 2012, doi: 10.1002/9781119941842.

[24]   P. U. Reddy, S. Sivanagaraju, and P. Sangameswararaju, "Power flow analysis of three phase unbalanced radial distribution system," *International Journal of Advances in Engineering & Technology*, vol. 514, pp. 514–524, 2012.

[25]   R. T. Ganesh Vulasala, Sivanagaraju Sirigiri, "Feeder reconfiguration for loss reduction in unbalanced distribution system using genetic algorithm," *International Journal of Electrical and Electronics Engineering*, vol. 3, no. 12, pp. 754–762, 2009.

BIOGRAPHIES OF AUTHORS

Ismail Yusuf [ID] [GS] [SC] [pub] obtained his Ph.D. in electrical engineering from Toyohashi University of Technology, Japan, in 2003. He joined the JSPS postdoctoral fellowship-Japan in 2005-2007. He is a professor at the Department of Electrical Engineering, Faculty of Engineering, Tanjungpura University, Indonesia. He is also head of the Energy Research Center at Tanjungpura University. His research interests include applications of wind and solar energy, power quality, and energy management system. He can be contacted at email: ismail.yusuf@ee.untan.ac.id.

Rudy Gianto [ID] [GS] [SC] [pub] received Ph.D. degree from The University of Western Australia in 2009. Currently, he is a Professor at Department of Electrical Engineering, Faculty of Engineering, Tanjungpura University, Indonesia. He is also head of Power and Distribution System Laboratory at Tanjungpura University. His research interests include power system analysis, simulation of power system dynamics, and distributed generation. He can be contacted at email: rudy.gianto@ee.untan.ac.id.